

## **Insights into thermal-assisted photocatalytic overall water splitting over ZnTi-LDH in a gas-solid reaction system**

Wang Xiaoning<sup>a, #</sup>, Chen Haowen<sup>a, #</sup>, Wang Kang<sup>b, \*</sup> and Wang Xitao<sup>a, \*</sup>

# These authors contributed equally to this work

\*Corresponding Author,

E-mail address: [wangk72@tju.edu.cn](mailto:wangk72@tju.edu.cn) (Kang Wang); [wangxt@tju.edu.cn](mailto:wangxt@tju.edu.cn) (Xitao Wang).

a. Tianjin Key Laboratory of Applied Catalysis Science and Technology,  
School of Chemical Engineering and Technology,  
Tianjin University, Tianjin 300072, China

b. Tianjin Key Laboratory of Membrane Science and Desalination Technology,  
Chemical Engineering Research Center, College of Chemical Engineering and  
Technology,  
Tianjin University, Tianjin 300072, China.

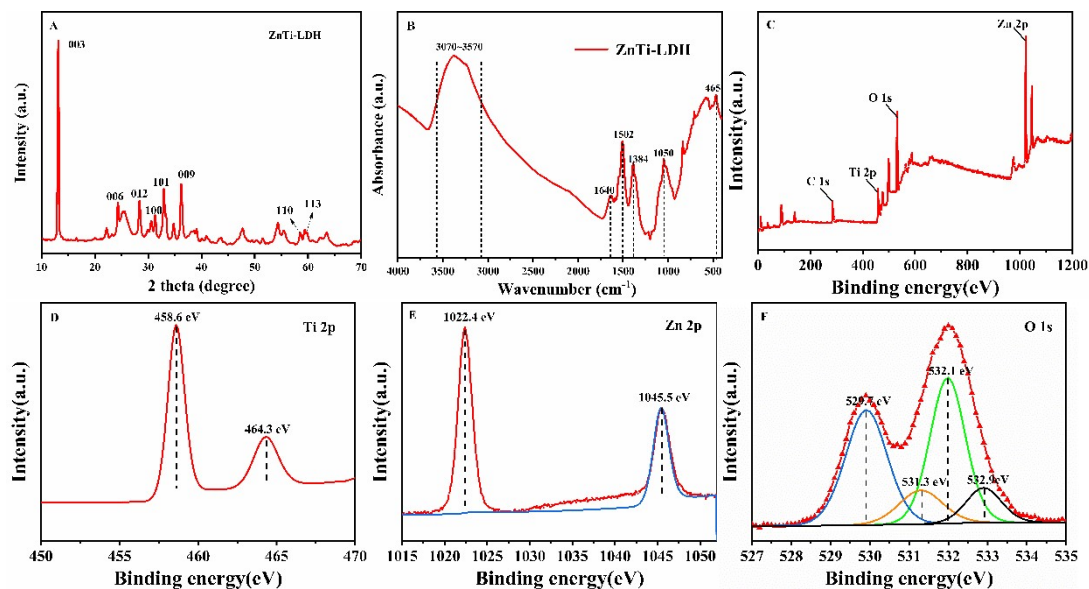


**Fig. S1.** (A) XRD patterns, (B) FT-IR spectra, (C) XPS full spectra, (D) Ti 2p spectra, (E) Zn 2p spectra and (F) O 1s spectra of ZnTi-LDH

As shown in Fig. S1. (A), the XRD pattern of ZnTi-LDH showed reflections of (003), (006), (009), (100), (101), (012), (110) and (113), which can be attributed to typical LDH materials[1]. The FT-IR spectra of ZnTi-LDH shown in Fig. S1. (B) displayed a strong broad absorption band at  $3070\text{ cm}^{-1}\sim 3570\text{ cm}^{-1}$ , which can be attributed to the OH stretching mode of interlayer water molecules and layer hydroxyl groups[2]. The band at  $1384\text{ cm}^{-1}$  and  $1502\text{ cm}^{-1}$  was assigned to mode  $\nu_3$  of interlayer carbonate species[3]. The band at  $1640\text{ cm}^{-1}$ ,  $1050\text{ cm}^{-1}$ ,  $465\text{ cm}^{-1}$  can be assigned to H-O-H bending vibration, M-O vibration modes of LDHs, O-M-O vibration related to LDHs layers, respectively[4]. The above confirmed the successful synthesis of ZnTi-LDH. As shown in Fig.S1. (C), the wide-scan XPS spectra of ZnTi-LDH confirm the existence of Ti, Zn, O and C, indicating the presence of ZnTi-LDH. The high-resolution XPS spectra of Ti 2p and Zn 2p (Fig. 3(b) and 3(c)) were fitted with two peaks, separately, and the peaks at 458.6 eV, 464.3 eV, 1022.4 eV and 1045.5 eV were assigned to Ti  $2p_{3/2}$ , Ti  $2p_{1/2}$ , Zn  $2p_{1/2}$ , and Zn  $2p_{3/2}$  for ZnTi-LDH[28]. The O 1s XPS spectra shown in Fig. 3(d) showed peaks at 532.9 eV, 532.1 eV, 531.3 eV and 529.7 eV which can be attributed to C-O functional group, adsorbed water, OH groups and lattice oxygen,

respectively[23]. All of the peaks agree well with those of ZnTi-LDH published in the literature [23,28].

As seen in Fig. S2(a, b), the structure of ZnTi-LDH was composed by irregular lamellar with lateral dimension of 100-120 nm. The HRTEM micrograph shown in Fig. S2 (d) indicated the single-crystalline nature of ZnTi-LDH. The lattice fringes with the lattice spacing of 0.25 nm was observed, which can be corresponded to the (009) plane of the ZnTi-LDH phase. The value was in conformity to the in-plane structural parameter of ZnTi-LDH ( $d_{009}=0.25$  nm) crystal determined from the XRD characterization.

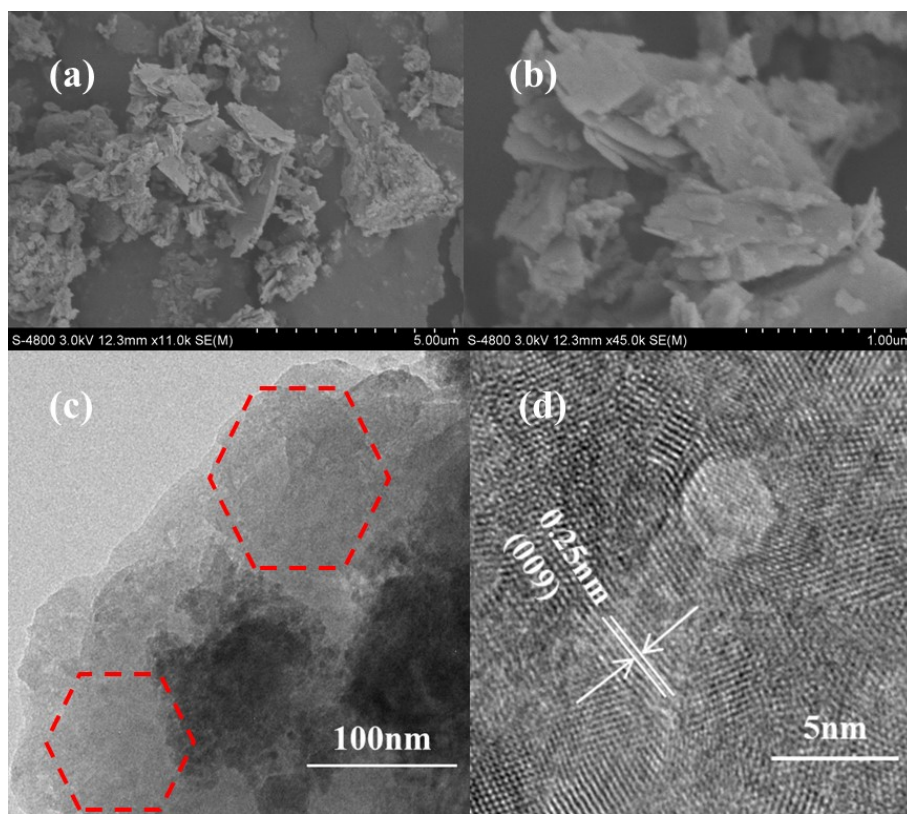
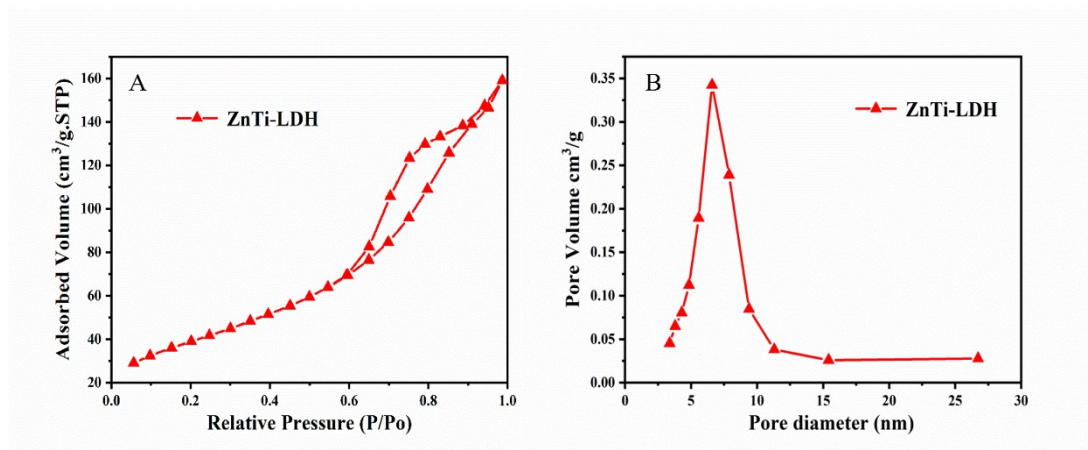
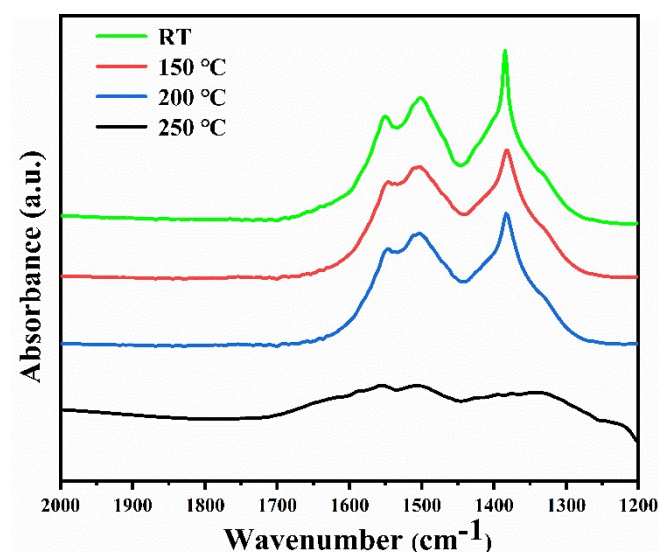


Fig. S2 (a, b) SEM image, (c) TEM image and (d) HRTEM image of ZnTi-LDH



**Fig.S3.** (A)  $N_2$  sorption isotherms and (B) pore size distribution of ZnTi-LDH



**Fig. S4.** FTIR spectra of ZnTi-LDH after the photocatalytic reaction at different temperatures

FTIR spectra of ZnTi-LDH after photocatalytic reaction at different temperatures were shown in Fig. S4. It can be seen clearly that the bands assigned to interlayer carbonate species were declined obviously at 250 °C, demonstrating the carbonate species have decomposed and the interlayer structure of the ZnTi-LDH has collapsed to some extent.

Table S1 Summary of LDH- based nanomaterials for photocatalytic water splitting

LDH-based semiconductors	Preparation method	Light source	Reaction time/temp erature	Sacrificial agent	H <sub>2</sub> evolution	Ref.
MgCr-LDH	Coprecipitation	125 W Hg Lamp $\lambda \geq 400$ nm	2 h/10 °C	10% MeOH	840 $\mu\text{mol g}^{-1} \text{h}^{-1}$	50
GaZn-ON	GaZn-LDH Coprecipitation	100 W high pressure USHIO	12 h/25 °C	Pure water	84 $\mu\text{mol g}^{-1} \text{h}^{-1}$	51
MgAl-LDH/NiS	Hydrothermal	300 W Xe lamp $\lambda > 420$ nm	3 h/6 °C	25 % MeOH	36 $\mu\text{mol g}^{-1} \text{h}^{-1}$	52
ZnGr-LDH/g-C <sub>3</sub> N <sub>4</sub>	Coprecipitation	300 W Xe lamp $\lambda > 420$ nm	8 h/25 °C	10% TEOA	187 $\mu\text{mol g}^{-1} \text{h}^{-1}$	53
CdS/NiFe-LDH	Microemulsion systems	300 W Xe lamp $\lambda > 420$ nm	3 h/25 °C	10% MeOH	469 $\mu\text{mol g}^{-1} \text{h}^{-1}$	54
ZnTi-LDH	Hydrothermal	300 W Xe lamp $\lambda > 420$ nm 200°C	4 h/250 °C	Pure water	322 $\mu\text{mol g}^{-1} \text{h}^{-1}$	In this work

50. S. Nayak, A. C. Pradhan, and K. M. Parida, *Inorganic Chemistry*, 2018, **57**, 8646-8661.
51. B. Adeli, F. Taghipour, *Applied Catalysis A: General*, 2016, **521**, 250-258.
52. J. Chen, C. Wang, Y. Zhang, Z. Guo, Y. Luo, C. Mao, *Applied Surface Science*, 2020, **506**, 144999.
53. B. Luo, R. Song, D. Jing, *International Journal of Hydrogen Energy*, 2017, **42**, 23427-23436.
54. H. Zhou, Y. Song, Y. Liu, H. Li, W. Li, Z. Chang, *International Journal of Hydrogen Energy*, 2018, **43**, 14328-14336.